



## RESEARCH ARTICLE

# A rational approach to improving titer in *Escherichia coli*-based cell-free protein synthesis reactions

Noelle Colant<sup>1</sup>  | Beatrice Melinek<sup>1</sup> | Jaime Teneb<sup>1</sup> | Stephen Goldrick<sup>1</sup> | William Rosenberg<sup>2</sup> | Stefanie Frank<sup>1</sup> | Daniel G. Bracewell<sup>1</sup> 

<sup>1</sup>Department of Biochemical Engineering, University College London, London, UK

<sup>2</sup>UCL Institute for Liver and Digestive Health, Division of Medicine, Royal Free Campus, London, UK

**Correspondence**

Daniel G. Bracewell, Department of Biochemical Engineering, University College London, WC1E 6BT London, UK.  
Email: d.bracewell@ucl.ac.uk

**Funding information**

Engineering and Physical Sciences Research Council, Grant/Award Number: EP/P006485/1

**Abstract**

Cell-free protein synthesis (CFPS) is an established method for rapid recombinant protein production. Advantages like short synthesis times and an open reaction environment make CFPS a desirable platform for new and difficult-to-express products. Most recently, interest has grown in using the technology to make larger amounts of material. This has been driven through a variety of reasons from making site specific antibody drug conjugates, to emergency response, to the safe manufacture of toxic biological products. We therefore need robust methods to determine the appropriate reaction conditions for product expression in CFPS. Here we propose a process development strategy for *Escherichia coli* lysate-based CFPS reactions that can be completed in as little as 48 hr. We observed the most dramatic increases in titer were due to the *E. coli* strain for the cell extract. Therefore, we recommend identifying a high-producing cell extract for the product of interest as a first step. Next, we manipulated the plasmid concentration, amount of extract, temperature, concentrated reaction mix pH levels, and length of reaction. The influence of these process parameters on titer was evaluated through multivariate data analysis. The process parameters with the highest impact on titer were subsequently included in a design of experiments to determine the conditions that increased titer the most in the design space. This proposed process development strategy resulted in superfolder green fluorescent protein titers of 0.686 g/L, a 38% improvement on the standard operating conditions, and hepatitis B core antigen titers of 0.386 g/L, a 190% improvement.

**KEYWORDS**

cell-free protein synthesis, multivariate data analysis, process development

## 1 | INTRODUCTION

Cell-free protein synthesis (CFPS) first emerged in the 1960s as part of research uncovering the genetic code.<sup>1</sup> Subsequently, this in vitro production method has been adapted to produce a variety of products including antibodies, biotherapeutic peptides, fusion proteins, vaccine

candidates, membrane proteins, toxic proteins, and bacteriophages.<sup>2</sup> There are broadly two types of CFPS: reconstituted CFPS and crude lysate CFPS. In reconstituted CFPS, also known as the Protein synthesis Using Recombinant Elements (PURE) system, purified recombinant proteins and ribosomes are added to the reaction in a bottom-up approach.<sup>3</sup> In crude lysate CFPS, a top-down approach is used in which

This is an open access article under the terms of the Creative Commons Attribution License, which permits use, distribution and reproduction in any medium, provided the original work is properly cited.

© 2020 The Authors. *Biotechnology Progress* published by Wiley Periodicals LLC on behalf of American Institute of Chemical Engineers.

cells are lysed and the extract clarified. In both systems, this extract is then combined with a concentrated reaction mix containing nucleotides, amino acids, energy substrates, salts, molecular crowding agents, polymerases, and genetic material for the expression of the product of interest. Cell extracts have been generated from a variety of host organisms: archaea, *E. coli*, yeast like *Saccharomyces cerevisiae* and *Pichia pastoris*, mammalian cells like Chinese hamster ovary, HEK293, and HeLa, wheat germ, and tobacco.<sup>4-6</sup> In this study, we used *E. coli*-based CFPS; in addition to being one of the more economical options, it is the most well-studied cell extract with dozens of publications to date and several commercial kits available on the market.

Transcription and translation are more streamlined in CFPS reactions because energy resources no longer need to be used to maintain metabolic activity for cell growth, though the protein synthesis rate is 200-fold slower than the *in vivo* rate.<sup>7</sup> The reactions are much shorter than *in vivo* cultivations, typically taking only a few hours. Titers of 2.3 mg/ml deGFP have been achieved with an *E. coli*-based CFPS system in batch mode in 10 hr.<sup>8</sup> Also, due to the absence of compartmentalized cells, CFPS reactions are open to additional components, like chaperones and detergents, which can easily be supplemented into the reaction to assist in protein folding and post-translational modifications.<sup>9,10</sup> When combined with orthogonal transfer RNAs, elongation factor Tu, and *E. coli* strains where release factor 1 has been eliminated, this open environment allows for the incorporation of nonnatural amino acids while maintaining high protein titers.<sup>11</sup> Several different formats have been used for the CFPS reaction including batch, fed-batch, microfluidic devices, and continuous-exchange reactions.<sup>12-15</sup> These reactions have been demonstrated to scale linearly in batch mode from the submilliliter scale to 100 L, a desirable characteristic for both the scale-up and scale-down of reactions.<sup>12</sup> Currently, Sutro Biopharma Inc. utilizes CFPS to manufacture an antibody drug conjugate with a nonnatural amino acid to allow for targeted conjugation to a specific site; the product is in clinical trials at present.<sup>16</sup> Recent work on lyophilized CFPS reactions has resulted in the development of “just-add-water” technologies, portable bioassays, environmental sensors, and paper-based sensors.<sup>17,18</sup> CFPS reactions have also been used for metabolic engineering and to observe gene circuits.<sup>18,19</sup>

Though CFPS has many advantages and applications, little work has been done on process development for these reactions. Current process development strategies for a typical biopharmaceutical in a mammalian cell host involves lengthy cell line development schemes that can take 60–90 days.<sup>20</sup> While this process may be shorter for microbial hosts like *E. coli* and *P. pastoris*, it is still cumbersome and requires cloning and selection from several strains. The fact that CFPS reactions can produce good titers in a shorter timescale and do not necessarily require any cloning steps, as PCR products can be used, allows for the use of high-throughput methodologies to design a process development strategy.<sup>21</sup>

We designed a process development strategy by examining the impact of process parameters, in particular cell extract strain, on product titer. Certain *E. coli* strains that have been engineered to have more stable mRNA or more eukaryotic tRNAs may result in better translation and increased yields for certain products. Similarly, we

have observed the impact of induction on product titer in isopropyl  $\beta$ -D-1-thioglycopyranoside (IPTG)-inducible BL21 Star™ (DE3) *E. coli* cells. Induction of the *E. coli* cells prior to extract preparation should result in an increased concentration of T7 RNA polymerase, an enzyme vital to transcription. Adding T7 RNA polymerase into the CFPS reaction is commonly found in the literature, as T7 RNA polymerase is highly selective for its own promoter sequences and it has a transcription rate that is higher than endogenous *E. coli* RNA polymerase.<sup>22</sup>

Because CFPS reaction conditions are no longer constrained by the needs of maintaining metabolically active cells, CFPS reaction parameters can be extended to greater extremes which may aid in the synthesis of difficult-to-express proteins and self-assembly processes (e.g., virus-like particles [VLPs]).<sup>23-25</sup> By adding more of the potentially limiting components for example, plasmid DNA or cell extract, the reaction equilibrium may be shifted to increase product yield. However, as both plasmid and extract preparation are time-consuming and labor-intensive processes, it is critical that the system not use more than what is required for either component. As the reactions are no longer limited by cell growth, the pH of the concentrated reaction mix can be decreased or increased far beyond typical physiological levels. However, pushing the pH of the reaction too far may have an adverse effect on the molecules required for transcription and translation of the product (ribosomes, polymerases, enzymes, and so forth) or could result in the precipitation of other reaction components. Because the polypeptide elongation rate in *E. coli* cells is enhanced at higher temperatures, increasing the reaction temperature should increase production, though too much of an increase may lead to protein degradation.<sup>26</sup> Additionally, lower temperatures may be beneficial as CFPS reactions are considered less thermostable than their corresponding host cells because they are more dilute; lower temperatures may also aid in protein folding and prevent aggregation.<sup>27</sup> The length of the reaction should be long enough to allow for the expression of high titers of protein but should not be so long that inhibitors like inorganic phosphate saturate the system.<sup>28</sup>

The work presented here investigates the impact of the aforementioned process parameters on product titer. We examined the *E. coli* strain used for the cell extract, two compositions of the concentrated reaction mix, and plasmid selection. We used multivariate data analysis (MVDA) to generate a model based on the titers resulting from reactions where the plasmid and cell extract concentration, pH of the concentrated reaction mix, reaction temperature, and length of reaction were manipulated individually. (We chose to compare two concentrated reaction mixture rather than investigate the individual components of the concentrated reaction mixtures because this has already been examined in some depth elsewhere.<sup>29,30</sup>) By performing a multilinear regression (MLR), we predicted which combination of parameters result in the highest titers within the robust operating space defined. The process parameters with the largest influence on titer were further evaluated through a response surface design of experiments (DoE) approach enabling the operating conditions that led to a significant increase in product titer to be identified. Several other groups have used DoE previously to examine multiple

parameters at once while using a minimal amount of reaction material in order to optimize parts of the CFPS system including extract preparation, chaperone and salt concentrations for expression of proteins with disulfide bonds, and the ratio of heavy chain expressing plasmid to light chain expressing plasmid for antibody expression.<sup>12,31-33</sup> Here we use DoE for titer maximization in a given design space, rather than optimization, to demonstrate how this process development strategy might be used with two different proteins.

## 2 | MATERIALS AND METHODS

All chemical reagents were purchased from Sigma-Aldrich (Dorset, UK) unless otherwise stated.

### 2.1 | Extract preparation

The extracts were derived from the BL21 (DE3) (Thermo Fisher Scientific, Paisley, UK), BL21 Star™ (DE3) (Thermo Fisher Scientific), and Rosetta™ (DE3) *E. coli* strains using the method outlined previously.<sup>34</sup> Briefly, a small volume, approximately 100  $\mu$ l, of bacterial glycerol stock was used to inoculate 50 ml fresh Lysogeny broth (LB) medium (pH 7.4) in a 250 ml baffled shake flask. The cultures were incubated overnight at 34°C and 250 rpm. The following day, approximately 16 hr later, 25 ml of the overnight culture was transferred to 500 ml of 2xYTPG medium pH 7.2 (16 g/L tryptone, 10 g/L yeast extract, 5 g/L NaCl, 7 g/L K<sub>2</sub>HPO<sub>4</sub>, 4.3 g/L KH<sub>2</sub>PO<sub>4</sub>, and 18 g/L glucose; adjusted pH to 7.2 with potassium hydroxide) in a 2 L baffled shake flask. The culture was incubated at 34°C and 220 rpm until OD<sub>600</sub>  $\approx$  2 was achieved at which point 500  $\mu$ l of 1 M potassium hydroxide was added to prevent acidification of the culture (as recommended by Hong et al. 2015) and the incubation continued.<sup>34</sup> When OD<sub>600</sub>  $\approx$  4 was achieved, the culture was harvested by centrifugation at 5,000 g and 4°C for 15 min; the cells should be entering stationary phase. Contrary to popular methods of harvesting during the mid-late log phase, Failmezger et al. showed that high performing extract can be produced from *E. coli* in the stationary phase; as such, we decided to simplify our workflow and adopt their method of extract production.<sup>35</sup> The supernatant was discarded and the pellets were kept on ice whenever possible. Each pellet was washed with  $\sim$ 25 ml of S30 buffer (pH 8.2 10 mM Tris acetate, 14 mM magnesium acetate, 60 mM potassium acetate, and 1 mM dithiothreitol) and resuspended by vortex. The resuspended cells were pelleted by centrifugation at 9,000 g and 4°C for 10 min. The pellet was washed, resuspended, and pelleted by centrifugation again. Excess supernatant was discarded. Pellets were stored at  $-80^{\circ}\text{C}$  following this step. Pellets were resuspended in 1.0 ml of S30 buffer per 1.0 g of pellet. The pellet was thawed on ice with S30 buffer for at least 1 hr prior to resuspension. The resuspended cells were homogenized via single pass at 1,000 bar through an APV Gaulin Micron Lab40 Homogenizer (Lubeck, Germany). The homogenized lysate was clarified by centrifugation at 30,000 g and 4°C for 30 min. The supernatant was recovered and

centrifuged again using the same conditions. The supernatant from the second centrifugation step was decanted and separated into 1 ml and 200  $\mu$ l aliquots. Aliquots were flash frozen with liquid nitrogen and stored at  $-80^{\circ}\text{C}$  until use.

The extract preparation method was not optimized or varied for different strains, as the authors have seen no evidence of any strain or product specific impact from extract preparation methods discussed in the literature. While we chose this protocol based on the equipment and reagents at our disposal, we recognize that numerous groups have thoroughly examined the extract preparation protocol and optimized conditions, such as length of time for cell growth, length of time for induction, and media for cell culture.<sup>31,36-39</sup>

In addition to the extracts prepared above, another BL21 Star™ (DE3) extract was prepared following the protocol above with the addition of 500  $\mu$ l of 1 M IPTG when the 500 ml shake flask cultivation had achieved OD<sub>600</sub>  $\approx$  0.6. This induction was done to increase the amount of T7 RNA polymerase in the extract. Unlike the other strains, these cells were incubated at 37°C.

A Bradford assay was used to determine total protein concentration for each extract; all extracts gave values of 30–50 mg/ml as expected based on the previous literature.<sup>40,41</sup> The total protein concentrations were as follows: 38 mg/ml for BL21 Star™ (DE3), 35 mg/ml for the BL21 (DE3), 34 mg/ml for Rosetta™ (DE3), and 44 mg/ml for the IPTG-induced BL21 Star™ (DE3).

### 2.2 | CFPS reaction

A cell-free concentrated reaction mix based on the protocol used by Kwon and Jewett (2015) was prepared.<sup>40</sup> The cell-free reaction included the following: 1.2 mM ATP, 0.85 mM each CTP, GTP, UTP, 1.5 mM spermidine, 1 mM putrescine, 33 mM phosphoenolpyruvate (PEP), 4 mM sodium oxalate, 0.27 mM coenzyme A (CoA), 0.33 mM nicotinamide adenine dinucleotide (NAD), 34  $\mu$ g/ml folinic acid, 170  $\mu$ g/ml tRNA from *E. coli* MRE 600, 90 mM potassium glutamate, 10 mM ammonium glutamate (MP Biomedicals, Eschwege, Germany), and 12 mM magnesium glutamate.<sup>40</sup>

Another concentrated reaction mix considered to be a simplified minimal mix based on the protocol by Cai et al. (2015) was also prepared.<sup>29</sup> This mix included the following: 1.2 mM AMP, 0.86 mM each CMP, GMP, UMP, 1.5 mM spermidine, 4 mM potassium oxalate, 15 mM phosphate buffer pH 7.0, 260 mM potassium glutamate, 8 mM magnesium glutamate, and 2 mM oxidized glutathione.<sup>29</sup> This mix is based on what is often referred to as the "Cytomim" mix because it was originally designed to mimic the cytosol environment in *E. coli* cells.<sup>42</sup> Instead of using expensive phosphorylated energy sources, this mix relies on oxidative phosphorylation and avoids the accumulation of inorganic phosphate and dramatic shifts in pH level over the course of the reaction.<sup>42,43</sup> The optimized version of this mix employed by Cai et al. (2015) reduced reagent costs by 95% while still producing over 1 g/L trastuzumab single-chain fragment variable.<sup>29</sup>

Each concentrated reaction mix was prepared as a 2.5 $\times$  concentrated solution (without amino acids or T7 RNA polymerase). Potassium

hydroxide was added to the complex concentrated reaction mix to solubilize the components. A volume of 2.5× concentrated reaction mix solutions were stored at  $-80^{\circ}\text{C}$  until use. A 75 mM methionine solution and a 50 mM solution containing the remaining amino acids were prepared separately and added to the reaction to a final concentration of 1.25 mM of each amino acid except methionine for which the final concentration was 1.5 mM. A total of 50 U/ $\mu\text{l}$  T7 RNA polymerase (Catalogue number: 18033019) was purchased from ThermoFisher Scientific™ and added to the reaction to a final concentration 500 U/ml T7 RNA polymerase. Amino acids solutions and T7 RNA polymerase were stored at  $-20^{\circ}\text{C}$  until use.

Reactions were performed in 100  $\mu\text{l}$  volumes in 1.5 ml microcentrifuge tubes from Star Labs (Milton Keynes, UK). In typical reactions, the concentrated reaction mix was combined with the amino acids solutions and T7 RNA polymerase as detailed above, 10  $\mu\text{g}/\text{ml}$  plasmid (6.1 nM for superfolder GFP [sfGFP], 2.8 nM for green fluorescent protein+ (GFP+), and 2.6 nM for Hepatitis B core antigen [HBcAg]), and 20% vol/vol cell extract, and then incubated at  $30^{\circ}\text{C}$  for 4.0 hr in an Eppendorf Thermomixer® C (Stevenage, UK) at 1,200 rpm. Reactions were analyzed for titer immediately and then stored at  $-20^{\circ}\text{C}$ .

## 2.3 | Adjusting continuous process parameters

Each of the following process parameters was examined in isolation in order to determine their impact on titer: plasmid concentration, amount of extract, temperature, pH of the concentrated reaction mix, and length. Plasmid concentration was adjusted by adjusting the volume of concentrated plasmid added to each reaction. Final concentrations of 1.0, 5.0, 10, 20, and 50  $\mu\text{g}/\text{mL}$  (0.61, 3.1, 6.1, 12.2, and 30.5 nM for sfGFP and 0.26, 1.3, 2.6, 5.1, and 12.8 nM for HBcAg) were prepared. Amount of extract was likewise adjusted by volume. Reactions with 5% vol/vol, 10% vol/vol, 15% vol/vol, 20% vol/vol, 25% vol/vol, 30% vol/vol, and 35% vol/vol extract were prepared. The pH level of 2.5× Kwon concentrated reaction mix was adjusted using small volumes of 18 M hydrochloric acid or 12 M sodium hydroxide. Below pH 5.5, the components began to fall out of solution. The following pH levels were tested: 5.0, 5.5, 6.0, 6.5, 6.8, 7.0, 7.5, 8.0, 8.5, and 9.0. Temperature was adjusted on each thermomixer; reactions at 15, 20, 25, 30, 32, 35, 37, and  $40^{\circ}\text{C}$  were tested. The following reaction lengths were assessed: 0.5, 1, 2, 4, 6, 8, 12, 22, and 24 hr. For sfGFP, the typical reactions conditions were 6.1 nM (10  $\mu\text{g}/\text{ml}$ ) plasmid, 20% vol/vol non-induced BL21 Star™ (DE3) extract, complex concentrated reaction mix at pH 6.8,  $20^{\circ}\text{C}$ , and 4 hr. Reactions adjusting the parameters were performed in triplicate and a total of 105 reactions were performed: typical reactions conditions (9 reactions), plasmid concentration at 4 levels (12 reactions), amount of extract at 6 levels (18 reactions), pH at 8 levels (24 reactions), temperature at 7 levels (21 reactions), and reaction length at 7 levels (21 reactions). Based on the sfGFP results, some reaction conditions were omitted for HBcAg. For HBcAg, the typical reaction conditions were 2.6 nM (10  $\mu\text{g}/\text{ml}$ ) plasmid, 20% vol/vol non-induced BL21 Star™ (DE3) extract, complex concentrated reaction mix at pH 6.0,  $20^{\circ}\text{C}$ , and 4 hr. Reactions were performed in duplicate and a total of 48 experiments were performed: typical reaction conditions (2 reactions), plasmid

concentration at 4 levels (8 reactions), amount of extract at 5 levels (10 reactions), pH at 4 levels (8 reactions), temperature at 4 levels (8 reactions), and reaction length at 6 levels (12 reactions).

## 2.4 | Design of Experiments

Following the “one-variable-at-a-time” analysis detailed in the previous section, a response surface DoE study was performed for each product to better understand the interactions between different process parameters and the subsequent impact on titer. This exercise was done to demonstrate how titer might be maximized using response surface DoE and validate its use as part of this process development strategy. It is not the intention to optimize titer, though that could be done by expanding the design space in subsequent DoE studies. A different DoE approach was used for each of the two products. For sfGFP, a face-centered central composite design consisting of nine runs with two center points was used. The following conditions were chosen: temperature of 32, 34, and  $36^{\circ}\text{C}$ ; pH of concentrated reaction mix of 5.5, 6.0, and 6.5. BL21 Star™ extract was used with 6.1 nM (10  $\mu\text{g}/\text{ml}$ ) plasmid and 20% vol/vol cell extract for 4.0 hr. For HBcAg, a face-centered central composite design consisting of 27 runs with 2 center points was used. The following conditions were chosen: temperature of 32, 34,  $36^{\circ}\text{C}$ ; plasmid concentration of 3.8, 7.7, 11.5 nM (15, 30, 45  $\mu\text{g}/\text{ml}$ ); amount extract of 15% vol/vol, 20% vol/vol, 25% vol/vol. These reactions were performed with an induced BL21 Star™ extract with pH 7.0 concentrated reaction mix for 4.0 hr.

## 2.5 | GFP plasmids

Commercial CFPS kit suppliers recommend using a plasmid which has been optimized for cell-free expression though plasmids typically employed for cell-based expression can be used as well.<sup>44</sup> Two GFP plasmids were selected: pJL1, a superfolder GFP plasmid, pJL1 was a gift from Michael Jewett (Addgene plasmid # 69496; <http://n2t.net/addgene:69496>; RRID:Addgene\_69,496), and pET14b-GFP, a plasmid developed by Martin Warren's group at the University of Kent used for *E. coli* expression of GFP+ with a 6xhistidine tag. Plasmid pJL1 has been optimized for CFPS. It is a much smaller plasmid (2,486 bp) that contains only the gene of interest (sfGFP in this case), the T7 promoter, the T7 terminator, a gene for kanamycin resistance and an origin of replication. The pET14b-GFP plasmid has not been optimized for cell free and has not been codon-optimized for *E. coli*. It is also somewhat large compared to the pJL1 plasmid, 5,389 bp.

## 2.6 | GFP analysis

For GFP analysis, it is assumed that all GFP proteins that have been produced are correctly folded and emit with the characteristic fluorescence intensity for that GFP variant. Titer was measured through fluorescence intensity measurement on a BMG Labtech (Aylesbury, UK)

FLUOStar OPTIMA spectrophotometer at an excitation wavelength of 485 nm and an emission wavelength of 520 nm and compared to a standard curve of rTurbo GFP from Evrogen (Moscow, Russia). The range of the standard curve was 80–1.6 µg/ml. To dilute into this range, all CFPS reactions were diluted 10-fold (20% vol/vol non-induced BL21 Star™ cell extract diluted in reverse osmosis water) For different GFP variants, fluorescence intensity was scaled based on quantum yield and extinction coefficient using the following equation where “ $F$ ” is the measured fluorescence of a sample, “ $\varphi$ ” is the quantum yield for that variant, “ $I_0$ ” is the intensity of the incident light, “ $\epsilon$ ” is the extinction coefficient for that variant, “ $l$ ” is the optical path length, and “ $c$ ” is the concentration of a sample.

$$F = \varphi I_0 (1 - 10^{-\epsilon lc})$$

The quantum yields for rTurbo GFP, sfGFP, and GFP+ are 0.53, 0.65, and 0.72, respectively.<sup>45–47</sup> The extinction coefficients for rTurbo GFP, sfGFP, and GFP+ are 70,000, 83,300, and 82,400 M<sup>-1</sup> cm<sup>-1</sup>, respectively.<sup>45–47</sup>

CFPS GFP samples were also analyzed via sodium dodecyl sulfate polyacrylamide gel electrophoresis (SDS-PAGE). Samples were reduced with NuPAGE Sample Reducing Agent (Thermo Fisher Scientific) and NuPAGE MES Sample Buffer (Thermo Fisher Scientific). The samples were not boiled because that would completely denature the protein and destroy fluorescence; previous groups have used this method to visualize fluorescent proteins in SDS-PAGE gels.<sup>48</sup> Samples were diluted four-fold with reverse osmosis water and the appropriate buffers and then applied to the lanes of a NuPAGE 12% Bis-Tris gel (Thermo Fisher Scientific) at 200 V for 50 min. Gels were imaged under blue fluorescent light (460 nm) on the GE Amersham™ Imager 600 (Pittsburgh, PA). The gels were then stained with InstantBlue™ Coomassie Protein Stain and imaged again under white light.

## 2.7 | HBcAg plasmid

The plasmid for the HBcAg dimer was obtained from iQur Ltd.<sup>49</sup> It is a plasmid for monomeric HBcAg subtype ayw under the T7 promoter in a pETDuet-1 backbone. Its exact sequence is unknown, but it is ~5,900 bp long. This plasmid has been used previously in vivo; it was not optimized for CFPS.

## 2.8 | HBcAg analysis

For HBcAg analysis, western blots and enzyme-linked immunosorbent assays (ELISAs) were used. For the western blots, samples were reduced with NuPAGE Sample Reducing Agent and NuPAGE MES Sample Buffer and boiled at 90°C for 10 min. Samples were diluted two-fold with reverse osmosis water and the appropriate buffers and then applied to the lanes of a NuPAGE 12% Bis-Tris gel at 200 V for 50 min. Proteins were transferred from the gel to a nitrocellulose membrane

using the Bio-Rad Trans-Blot® Turbo™ Transfer System (Hercules, CA). The membrane was blocked in TBST-M before incubation with the primary antibody: anti-hepatitis B virus core antigen antibody [10E11] (Abcam, Cambridge, UK). The membrane was washed with tris-buffered saline with Tween 20 (TBST) and then incubated with the secondary antibody: goat anti-mouse horseradish peroxidase (HRP)-conjugated antibody [HAF007] (R&D Systems, Abingdon, UK). The membrane was washed with TBST. A final wash with tris-buffered saline (TBS) was performed before applying the Thermo Fisher Scientific Pierce ECL Western Blotting Substrate. The membrane was imaged under chemiluminescent light on the GE Amersham™ Imager 600.

For the ELISAs, the QuickTiter™ Hepatitis B Core Antigen (HBVcAg) ELISA Kit from Cell Biolabs (San Diego, CA) was used according to the recommended protocol.

The particles were also purified via ammonium sulfate precipitation. The soluble fraction obtained from the reaction was incubated with 1.9 M ammonium sulfate for 5 min. After the particles were pelleted by centrifugation at 15,000 g for 10 min, they were resuspended in 0.1 M Tris buffer pH 8.7, 1 mM EDTA, 0.15 M NaCl. The samples were filtered using 0.22 µm Costar® Spin-x® centrifuge tube filters from Corning (Flintshire, UK). The samples were applied to a carbon/formvar-coated copper 300 mesh grids purchased from Generon (Slough, UK) for 1 min. The grid was washed with water for 5 s and then negatively stained with 2% uranyl acetate in water for 30 s. The grids were imaged under a JEOL JEM-1010 transmission electron microscope (TEM) (Welwyn Garden City, UK) and imaged under a Gatan Orius camera (Abingdon, UK).

## 2.9 | Multivariate data analysis

MVDA was used to evaluate the results from the reactions detailed in Materials and Methods (Section 2) to determine which combination of conditions would maximize titer and to gain a better understanding of each variable's contribution on titer for both products investigated. Data manipulation and analysis for the MLR model was performed using MatLab R2019b (MathWorks, Inc., Natick, MA). MLR was used to predict a single dependent variable—titer—from a series of independent inputs—plasmid concentration, amount of *E. coli* extract in the reaction, pH of concentrated reaction mix, temperature of reaction, and length of reaction. In this manner, the contribution of each independent parameter on titer can also be determined. The variables of importance were found by creating multiple MLR models that studied the influence of each parameter that was removed during the development of models that considered linear, quadratic, polynomial (squared terms and cubed terms), and interactions. Separate models were created for sfGFP and HBcAg titers. The prediction performance of the MLR was quantified using the coefficient of determination, which is calculated as:

$$R^2 = \frac{\sum (\hat{y}_i - \bar{y})^2}{\sum (y_i - \bar{y})^2}$$

where,  $y_i$  is the product concentration for run  $i$ ,  $\bar{y}$  is the product concentration mean, and  $\hat{y}_i$  is the predicted product concentration for run

i. The MLR model terms were chosen based on a stepwise regression approach implementing both forward addition and backward elimination of terms based on their  $p$ -value which ensured a robust and statistically valid model. The selection criteria for the finalized model was based on maximizing the coefficient of determination between the model predictions and the experimental product concentrations.

### 3 | RESULTS AND DISCUSSION

#### 3.1 | Establishing a working CFPS system

In order to increase titer in our CFPS system, we first need to design a CFPS system to establish a baseline. We considered three major components of system: plasmid selection, the concentrated reaction mixture composition, and the *E. coli* strain of the cell extract. We trialed two plasmids: pJL1, a CFPS-optimized plasmid created by the Jewett Lab at Northwestern University for sfGFP production, and pET14b-GFP, a plasmid design for in vivo expression of GFP+ with a 6×histidine tag originally developed by Martin Warren's group at the University of Kent. Both plasmids were used in CFPS reactions at a concentration of 3 nM where all other conditions were the same. The non-induced BL21 Star™ (DE3) extract and the complex concentrated reaction mix based on the protocol in Kwon and Jewett (2015) were used. The reactions were analyzed based on sfGFP and GFP+ production.

The reactions with the pJL1 plasmid achieved over double the titer achieved with the reactions using the pET14b-GFP plasmid: an

average of 227  $\mu\text{g}/\text{mL}$  compared to an average of 106  $\mu\text{g}/\text{mL}$  (Figure 1a). This demonstrates that traditional plasmids may not perform as well as a plasmid optimized for CFPS. Care should be taken, however, not to assume that this is generally true.<sup>50-53</sup> The pJL1 plasmid expresses sfGFP, which folds more readily and is brighter than the GFP+ produced using the pET14b-GFP plasmid.<sup>54,55</sup> Though we have corrected for this, the fluorescence readings for sfGFP are generally stronger. In addition, using plasmid preparation kits, we are usually able to produce more pJL1 plasmid (~400–500  $\text{ng}/\mu\text{L}$ , ~240–300 nM) than pET14b-GFP plasmid (~150–250  $\text{ng}/\mu\text{L}$ , ~40–55 nM). We chose to use the pJL1 plasmid for the subsequent experiments involving GFP for the sake of easier detection and easier plasmid preparation. The value in first screening alternative plasmids comes also from the need to confirm the quality of the plasmids and their suitability for in vitro transcription and translation before undertaking the more extensive range of experiments which follow; it has been seen for example, that plasmid purification may have a substantial effect on subsequent in vitro reactions.<sup>56</sup>

Next we prepared two concentrated reaction mixes, a complex mix based on the work shown in Kwon and Jewett (2015) and a minimal mix based on the work shown in Cai et al. (2015).<sup>29,40</sup> For the CFPS reactions, these concentrated reaction mixes were combined with the non-induced BL21 Star™ (DE3) extract and 6.1 nM (10  $\mu\text{g}/\text{mL}$ ) of the pJL1 plasmid. The reactions were analyzed based on sfGFP production. The complex mix gave titers over three times greater than the minimal mix, an average of 497  $\mu\text{g}/\text{mL}$  compared to an average of 146  $\mu\text{g}/\text{mL}$  (Figure 1b). This may be due to a depletion of energy

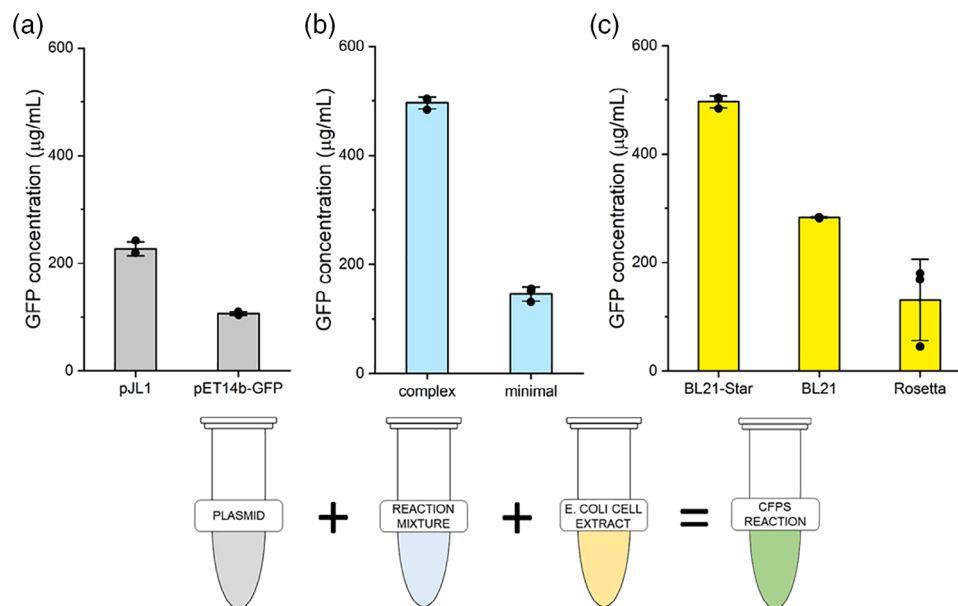


**FIGURE 1** CFPS *Escherichia coli* plasmid, concentrated reaction mix, and extract comparison (a) 3 nM of the pJL1 plasmid and the pET14b-GFP plasmid combined with the BL21 Star™ (DE3) extract and the complex concentrated reaction mix based on the protocol in Kwon and Jewett (2015).<sup>40</sup> (b) The complex concentrated reaction mix and a minimal concentrated reaction mix based on the protocol in Cai et al. (2015)<sup>29</sup> were prepared and combined with the BL21 Star™ (DE3) extract and the pJL1 plasmid. (c) Extracts were prepared from four different strains and combined with concentrated reaction mix based on Kwon et al. (2015)<sup>40</sup> and the pJL1 plasmid. Error bars represent plus or minus one SD for  $n = 3$  biological replicates, each represented as a single data point. In typical reactions, the concentrated reaction mix was combined with 6.1 nM (10  $\mu\text{g}/\text{mL}$ ) pJL1 plasmid and 20% vol/vol cell extract and then incubated at 30°C for 4.0 hr. CFPS, cell-free protein synthesis

sources in the minimal mix; the complex mix contains more energy sources, in particular PEP, CoA, and NAD<sup>+</sup>, that may allow for prolonged ATP regeneration.<sup>30</sup> The complex mix also utilizes nucleotide triphosphates instead of nucleotide monophosphates, as used in the minimal mix, which may allow for better ATP regeneration as well as higher rates of transcription and translation, especially when paired with additional *E. coli* tRNAs, which are also absent from the concentrated minimal mix. However, it is worth noting that CFPS reactions have been shown to be able to generate nucleotide triphosphates from nucleotide monophosphates in both crude cell lysate CFPS and the PURE system.<sup>29,57</sup> Based on these results, the complex concentrated reaction mix was used in subsequent screening studies.

Then, we examined three different *E. coli* strains: BL21 (DE3), BL21 Star™ (DE3), and Rosetta™ (DE3) (Table 1).<sup>58</sup> The BL21 (DE3) strain is a widely used, high expression strain that allows for expression of recombinant genes under the T7 promoter. The BL21 Star™ (DE3) strain is a derivative of the BL21 (DE3) strain with reduced levels of endogenous RNases resulting in more stable mRNA and enhanced protein expression. The Rosetta™ (DE3) strain is a variation on the BL21 (DE3) strain that supplies tRNAs that are not naturally expressed at high levels in *E. coli* to allow for increased production of eukaryotic proteins.

The extracts were used in CFPS reactions with the concentrated reaction mix based on Kwon and Jewett (2015) and 6.1 nM (10 µg/ml) of the pJL1 plasmid. The reactions were analyzed based on sfGFP production. The highest titers, an average of 497 µg/ml sfGFP, were achieved with the BL21 Star™ (DE3) extract (Figure 1c). The BL21 (DE3) and Rosetta™ (DE3) extracts produced significantly less, 283 and 131 µg/ml, respectively. This suggests that mRNA stability plays a key role in protein production via CFPS, though significant protein production can still be achieved without the mutated RNase E found in BL21 Star™. The inclusion of eukaryotic tRNAs has an adverse effect on protein production, as seen with the Rosetta™ (DE3) extract. However, this extract may be useful for the production of other proteins of eukaryotic origin in future. Overall, the varied sfGFP titers achieved with the different strains suggests that choosing the appropriate strain for the product of interest is important to achieving high titers. Due to the high performance of the BL21 Star™ (DE3) extract, it was used in the subsequent screening studies.

**TABLE 1** *Escherichia coli* strains for extract preparation<sup>55</sup>

Bacterial strain	Features
BL21 (DE3)	Contains T7 polymerase upon IPTG induction; deficient of lon and omp-t proteases; suitable for expression of non-toxic genes
BL21 star™ (DE3)	Contains T7 polymerase upon IPTG induction; contains a mutated RNase E to reduce RNase degradation and boost protein expression
Rosetta™ (DE3)	Contains T7 polymerase upon IPTG induction; supplies tRNA for the codons AUA, AGG, AGA, CUA, CCC, and GGA to enhance expression of eukaryotic proteins

Abbreviation: IPTG, isopropyl β-D-1-thioglycopyranoside.

The BL21 (DE3) Star™ strain, as with all the DE3 strains used in this study, can be induced with IPTG to produce T7 RNA polymerase.<sup>59</sup> We therefore investigated the impact of IPTG induction during cell cultivation on cell extract performance. While constitutive promoters like σ<sup>70</sup> promoter can be used in CFPS, the gene of interest is under the T7 promoter in all the DNA plasmids used in this study.<sup>35,60</sup> Thus, T7 RNA polymerase results in the expression of the target gene. T7 RNA polymerase is an essential component in the CFPS reaction; by increasing the concentration present in the crude cell extract, the amount of this expensive reagent added to the reaction may be significantly decreased. An induced extract was prepared using the BL21 Star™ (DE3) strain and compared to the non-induced BL21 Star™ (DE3) strain, with and without additional exogenous T7 RNA polymerase in the reaction. The reactions were analyzed based on sfGFP production as measured based on fluorescence (Figure 2a) and further verified with a fluorescent-image of an SDS-PAGE (Figures 2b). It was demonstrated that induced strains do not require additional T7 RNA polymerase, but non-induced strains do require additional T7 RNA polymerase. However, induced strains, with and without the additional T7 RNA polymerase, gave somewhat lower titers—an average of 357 µg/ml with additional T7 RNA polymerase and 379 µg/ml without additional T7 RNA polymerase—than the non-induced with additional T7 RNA polymerase—an average of 497 µg/ml. It is important to be aware, however, of the substantial batch-to-batch variability which may be seen in extract production,<sup>56,61</sup> as shown by the three additional batches of IPTG-induced extract in Figure 2a. While the batch-to-batch variation is not unreasonable by current standards in the art, it is still substantial relative to the titer difference. Consequently, for the pJL1 plasmid the difference in titer between the induced and non-induced extract with addition of T7 RNA polymerase is not statistically significant. The non-induced BL21 Star™ (DE3) extract was used in subsequent experiments with the pJL1 plasmid.

### 3.2 | Comparison to a commercial CFPS system

Overall, the combination of extract, concentrated reaction mix, and plasmid that gave the highest average titer of sfGFP was the BL21 Star™ (DE3) extract, the complex concentrated reaction mix based on the protocol in Kwon and Jewett (2015) and 6.1 nM (10 µg/ml) of the pJL1 plasmid. This CFPS platform was compared to the commercial kit sold by ThermoFisher Scientific™, the Expressway™ Mini-Cell Free Expression System.<sup>44</sup> The reactions were analyzed based on sfGFP production. We found this platform, which gave an average titer of 497 µg/ml, performed as well as the commercial kit, which gave an average titer of 493 µg/ml (data not shown).

### 3.3 | Confirming the choice of extract for the second product: HBcAg

Now that we have established our CFPS system, we can manipulate various process parameters to improve product concentration and use

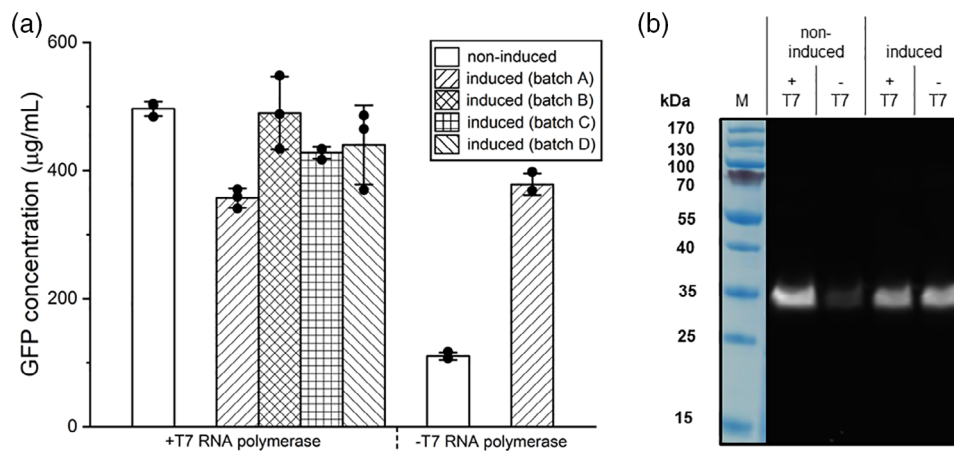


**FIGURE 2** IPTG-induced and non-induced BL21 Star™ (DE3) extracts with and without additional T7 RNA polymerase (a) A non-induced and an induced BL21 Star™ (DE3) extract were combined with the pJL1 plasmid and the reaction based on the protocol by Kwon and Jewett (2015)<sup>40</sup> with and without additional T7 RNA polymerase. Error bars represent plus or minus one SD for  $n = 3$  biological replicates, each represented as a single data point. Four different batches of induced BL21 Star™ (DE3) extract with additional T7 RNA polymerase are shown in the different patterned bars to illustrate batch-to-batch variation. (b) Image under fluorescent light of an SDS-PAGE analysis of non-induced BL21 Star™ (DE3) extract with and without additional T7 RNA polymerase and induced BL21 Star™ (DE3) extract with and without additional T7 RNA polymerase. Reactions were performed with the concentrated reaction mix based on the protocol from Kwon and Jewett (2015)<sup>40</sup> and the pJL1 plasmid. CFPS reaction samples were diluted 1:3 in reverse osmosis water, NuPAGE Sample Reducing Agent, and NuPAGE MES Sample Buffer. CFPS, cell-free protein synthesis; IPTG, isopropyl  $\beta$ -D-1-thioglycopyranoside; SDS-PAGE, sodium dodecyl sulfate polyacrylamide gel electrophoresis

this analysis to inform our process development strategy. We have chosen to demonstrate this strategy with two products, sfGFP and HBcAg VLPs. We have already determined the appropriate *E. coli* strain for the cell extract for sfGFP production, and before we can employ our process development strategy, we will need to do the same for HBcAg.

HBcAg production was observed in CFPS reactions with the four previously mentioned cell extracts (Figure 3a). We found that an induced extract is required for the production of consistent and strongly detectable titers of HBcAg. In fact, when non-induced and induced BL21 Star™ (DE3) extracts were used both with and without additional T7 RNA polymerase, two very different outcomes were observed (Figure 3b). Little to no expression was observed with the non-induced extract regardless of whether or not additional T7 RNA polymerase was used in the reaction. In reactions with the induced extract, HBcAg expression was easily detectable—again, whether or not additional T7 RNA polymerase was used in the reaction. Induced extracts should have a higher concentration of T7 RNA polymerase than non-induced extracts and would contain residual IPTG that would be found within the homogenized cell cytosol. This may be critical because the HBcAg gene is expressed from a pETDuet-1 plasmid and this plasmid contains the lac operator and the lac repressor gene (*lacI*) which normally inhibits transcription of the gene of interest. However, the inhibition is relieved when IPTG binds to LacI, and the gene of interest can be expressed. Alternatively, induction may result in other changes to the cellular components (ribosomes, elongation factors, initiation factors, release factors, and so forth) that may inherently improve protein expression, but that will depend upon the rate limiting step for a given protein/plasmid. Subsequent process parameter analysis was based on the results achieved using the IPTG-induced

BL21 Star™ extract. The purified particles were observed under TEM and demonstrated self-assembly (Figure 3c).

### 3.4 | Examining process parameters with two products: sfGFP and HBcAg

The influence of varying the following process parameters on sfGFP and HBcAg titers were examined: plasmid concentration, amount of extract, temperatures, pH of the concentrated reaction mix, and reaction lengths (Figure 4). Each parameter was initially examined in isolation. The initial values were chosen based off the recommendations made in the ThermoFisher Scientific™, the Expressway™ Mini-Cell Free Expression System handbook.<sup>44</sup> For a standard reaction producing sfGFP, the following conditions were used: 6.1 nM plasmid for sfGFP (10 µg/ml plasmid), 20% vol/vol extract, 30°C, a concentrated reaction mix at pH 6.8, and 4 hr long reaction. The BL21 Star™ (DE3) extract without IPTG induction, the complex concentrated reaction mix, and the pJL1-sfGFP plasmid were used. For a standard reaction producing HBcAg, the following conditions were used: 2.6 nM (10 µg/ml) pETDuet-1 plasmid for the expression of HBcAg monomer proteins, 20% vol/vol extract, 30°C, a concentrated reaction mix at pH 6.0, and 4 hr long reaction. The IPTG-induced BL21 Star™ (DE3) extract, the complex concentrated reaction mix, and the pETDuet-1 plasmid for HBcAg expression were used.

Commercial CFPS kits recommend 10 µg/ml plasmid and 20% vol/vol extract.<sup>44</sup> However, the processes for plasmid and extract preparation are laborious, time-consuming, and expensive. Therefore, minimizing the amount used in each reaction would enable more experimental conditions to be evaluated faster and more



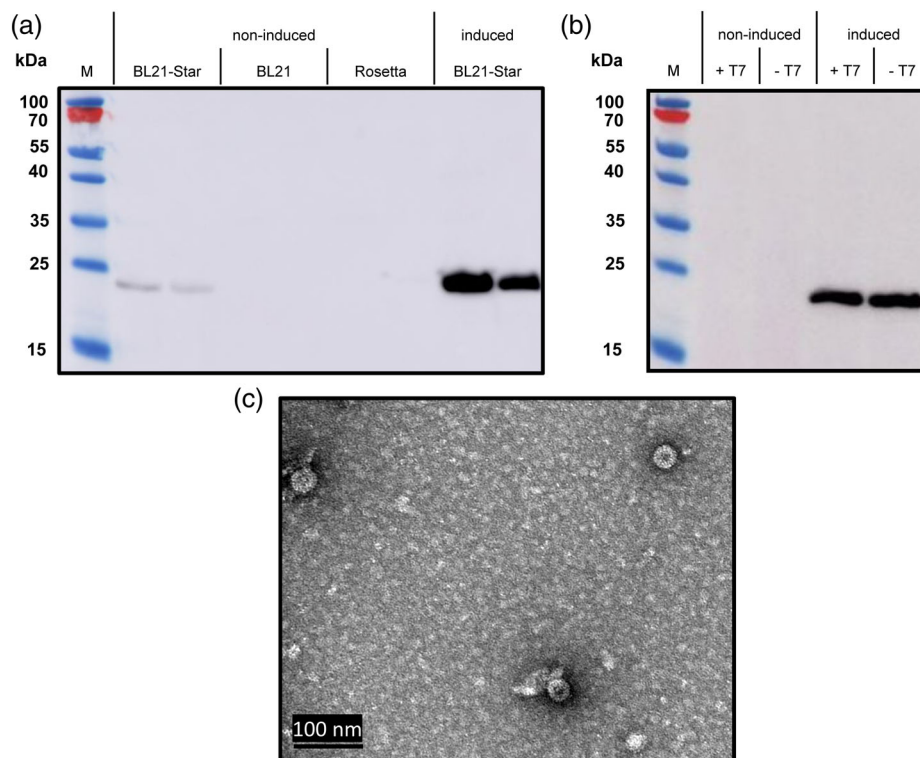


**FIGURE 3** Extract strain effects on HBcAg monomer titer. (a) Induced BL21 Star™ extract results in a higher product concentration of HBcAg monomer compared to other non-induced extracts. For each extract, the left lane is the CFPS reaction and the right lane is the soluble fraction from that reaction. (b) No production of HBcAg is observed in non-induced BL21 Star™ (DE3) extract regardless of whether or not additional T7 RNA polymerase is added to the reaction; production is observed with and without additional T7 RNA polymerase in reactions with an IPTG-induced BL21 Star™ (DE3) extract. The reactions run in (b) are separate from the ones run in (a) and the IPTG-induced BL21 Star™ (DE3) extract used in (b) is a different batch than the one used in (a) therefore representing biological replicates. (c) Assembled HBcAg VLPs imaged under TEM from the reaction with the following conditions: 2.6 nM (10 µg/ml) plasmid, 20% vol/vol extract, concentrated reaction mix pH 6.0, 30°C, and 4 hr. CFPS, cell-free protein synthesis; HBcAg, Hepatitis B core antigen; IPTG, isopropyl β-D-1-thiogalactopyranoside; VLPs, virus-like particles; TEM, transmission electron microscope

economically. If reactions with higher plasmid or extract concentrations resulted in significantly higher yields, this would be beneficial knowledge for process development. With that in mind, plasmid concentration ranges applied were from 0.61 nM (1 µg/ml) to 30.5 nM (50 µg/ml) for sfGFP reactions, and 0.26 nM (1 µg/ml) to 12.8 nM (50 µg/ml) for HBcAg reactions. For both products, the highest titers are achieved when a plasmid concentration of over 5 nM (10 µg/ml for sfGFP, 20 µg/ml for HBcAg) is used; the product concentrations plateau or decrease at higher plasmid concentrations (Figure 4a). A few research groups have examined plasmid concentration with a single product and determined that increasing the plasmid concentration can boost product concentration to a certain point, but other species involved in transcription and translation need to be replenished after that, namely tRNAs and T7 RNA polymerase.<sup>34,62,63</sup> It would seem that 5 nM of plasmid, regardless of the product, is the maximum amount our system can accommodate before other components must be manipulated to increase product concentration. Also, aside from the choice of using an induced extract over a non-induced extract, plasmid concentration was the process parameter which had the greatest impact on monomeric HBcAg titer, which may suggest the typical amount of plasmid used in the reaction (2.6 nM) is limiting.

Amount of extract from 5% vol/vol to 35% vol/vol was examined with sfGFP and 5% vol/vol to 30% vol/vol with HBcAg. Titers were relatively consistent (~450 µg/ml sfGFP and ~175 µg/ml HBcAg) when amount of extract was above 20% vol/vol (Figure 4b). It is likely that other resources (polymerases, amino acids, nucleotides, and so forth) are depleted and plasmid or extract is no longer the limiting reagent or that inhibitors like inorganic phosphate have accumulated.

Commercial kit suppliers recommend reaction temperatures between 30 and 37°C.<sup>44</sup> We expanded this range testing reactions at temperatures from 15 to 40°C for sfGFP and 20 to 35°C for HBcAg. Titers peaked with a reaction temperature of 32–35°C for both products (Figure 4c). Though 32–35°C may maximize sfGFP and HBcAg production, other products may require higher or lower temperatures. Lower temperatures might be preferable for more complex molecules with solubility issues as this tends to reduce the formation of inclusion bodies.<sup>64</sup>

Previous studies have indicated that pH is one of the most critical process parameters in CFPS reactions.<sup>41,65</sup> In sfGFP production, we also observed this to be true; as the pH of the concentrated reaction mix decreased, the product concentration increased (Figure 4d). Titers of over 700 µg/ml were achieved with a concentrated reaction mix of pH 5.5. This is likely because the other components in the CFPS

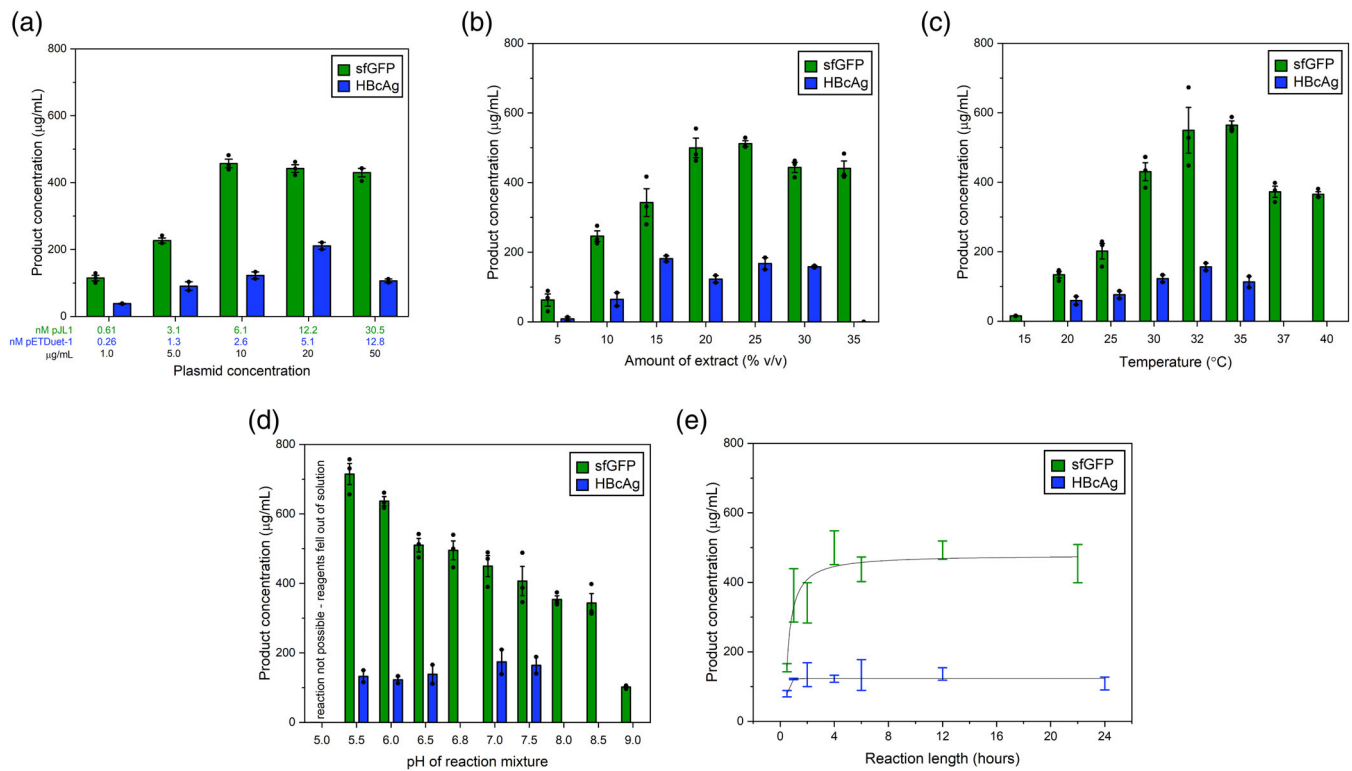


**FIGURE 4** Process parameter effects on sfGFP and HBcAg titer. Titers for sfGFP are shown in green and titers for HBcAg are shown in blue. (a) Product concentration increases with increasing plasmid concentration until 6.1 nM (10 µg/ml) for sfGFP and 5.1 nM (20 µg/ml) for HBcAg. (b) Likewise, product concentrations increase with increased amount of extract until 20% vol/vol for sfGFP and 15% vol/vol for HBcAg. (c) The highest product concentrations are seen at temperatures between 30 and 35°C for both products. (d) Product concentration increases with decreasing pH of the concentrated reaction mix for sfGFP and product concentration is not significantly affected by pH for HBcAg; pH 5.0 could not be achieved due to precipitation of the concentrated reaction mix components. (e) The maximum product concentration is achieved after 4 hr of reaction. For (a) through (d), error bars represent plus or minus one SE for  $n = 3$  biological replicates for sfGFP and  $n = 2$  biological replicates for HBcAg, each represented as a single data point. For (e) error bars represent plus or minus one SE for  $n = 3$  biological replicates for sfGFP and  $n = 2$  biological replicates for HBcAg. HBcAg, Hepatitis B core antigen; sfGFP, superfolder GFP

system are basic in nature, in particular the concentrated solution of amino acids that is added separately to the reaction, which must be kept at pH 12 in order to remain soluble.<sup>61</sup> By using the concentrated reaction mix to decrease the overall pH, the reaction as a whole was closer to a more neutral pH which may be ideal for the transcription and translation machinery in the extract. Reactions at even lower pH values might be achieved in the future by preparing the extract with an acidic buffer and minimizing the addition of base required to keep the amino acids in solution. Also, it is important to note in interpreting these results that while sfGFP is a pH sensitive protein, it has been demonstrated to display negligible differences in fluorescence intensity in the pH 5.3–9.4 range and the reaction is diluted 10-fold with 20% extract before measurement which should minimize the effects of the slight differences in overall pH between the reactions.<sup>66,67</sup> Unlike sfGFP, HBcAg titers were not greatly affected by a change in pH of the concentrated reaction mix (Figure 4d). For HBcAg, the titers all lie within 100 µg/ml of each other. This might indicate that reactions expressing HBcAg are limited by a component that is not particularly pH sensitive.

Reaction length is highly variable amongst previous studies: batch reactions from 2 to 24 hr have been examined.<sup>28,68</sup> In our own

studies, we observed a visible green tint to the CFPS reactions producing sfGFP after only 0.5 hr of incubation; therefore, we examined reaction lengths from 0.5 to 22 hr for sfGFP and 0.5 to 24 hr for HBcAg. In observing the length of the reactions, titers stabilized after 4 hr for both products (Figure 4e). However, as the length of the reaction increases, the variability in titer becomes much greater. Therefore, when possible shorter reaction times are recommended. Also, sfGFP is known to fold efficiently with good folding kinetics.<sup>54</sup> Other products with known assembly issues may require longer reaction times. Alternatively, certain amino acids and nucleotides may be depleted after 4 hr of reaction. To replenish these reagents, a concentrated solution of amino acids and nucleotides could be fed into the reaction or continuous reactions could be used instead of the batch method employed here.<sup>69</sup>

### 3.5 | MVDA to maximize product titer

It was difficult to quantify the influence of each variable on product concentration due to the complex interactions between all process parameters. Therefore, to quantify the relative importance of each

variable and their ability to predict the product concentration, four different types of MLR models were generated.

MVDA was selected to evaluate the screening design based on its proven ability within the biopharmaceutical sector to leverage useful information from complex data sets and uncover useful correlations that are not always obvious from univariate analysis.<sup>70</sup> The DoE methodology implemented is a systematic approach enabling the

relationship between process operation and process output to be determined while reducing the required number of experiments to understand these key relationships. The face-centered composite DoE was selected as it is the most appropriate design when factors investigated cannot be extended beyond the factorial points which was the case in this experiment. It also enables linear, interactive, and quadratic terms to be evaluated as it contains center points in addition

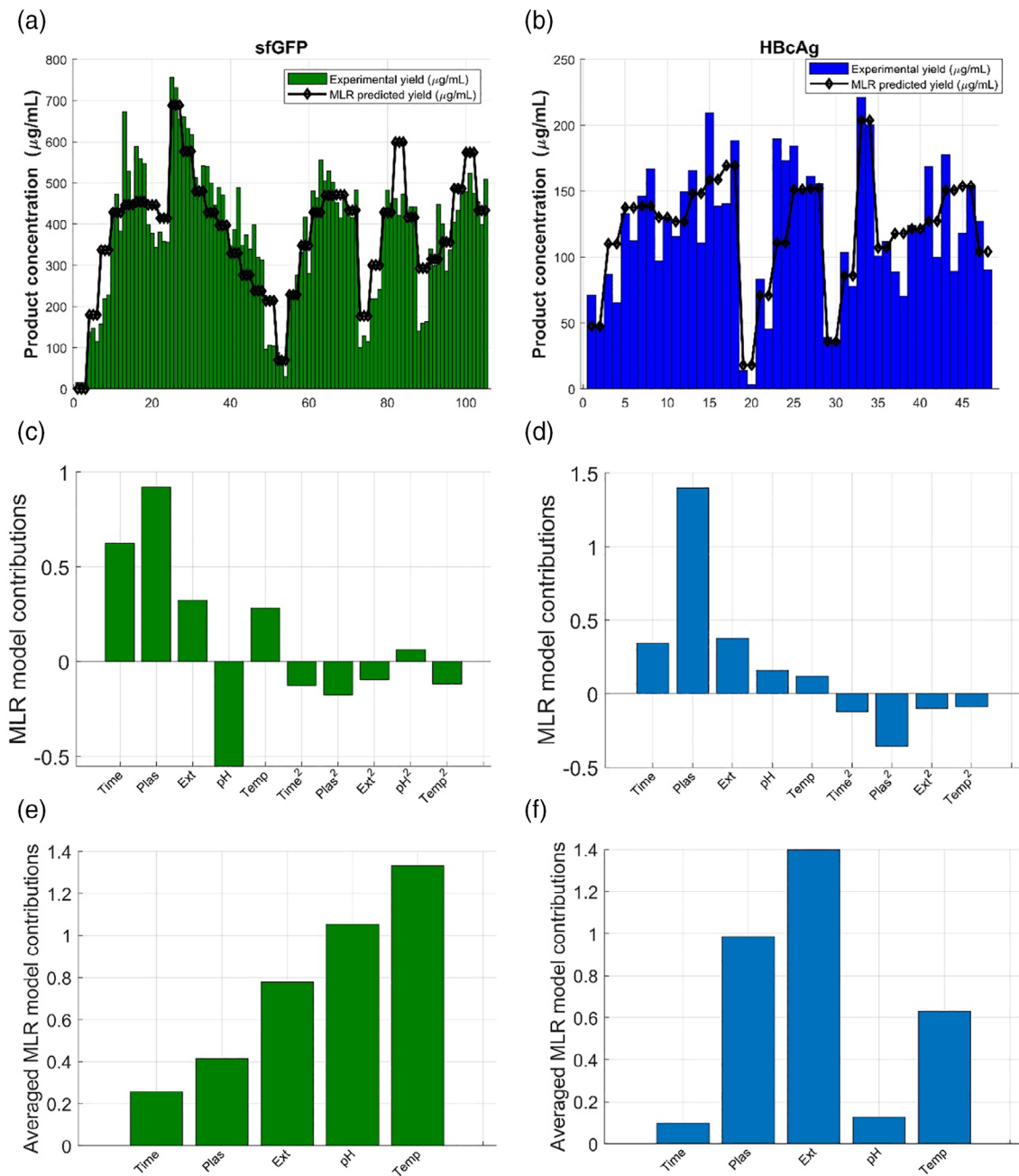


**FIGURE 5** Multivariate data analysis of process parameters. The MLR models for sfGFP and HBcAg titers, respectively, are shown in (a) and (b), where each bar represents the product concentration from an experimental run (the experimental runs are the same ones shown in Figure 4 and detailed in Table 2 and Table 3). The contributions of each parameter to titer is shown in (c) and (d), where “Time” is the length of the reaction “Plas” is the plasmid concentration, “Ext” is the amount of extract in the reaction, “pH” is the pH of the concentrated reaction mix, and “Temp” is the temperature of the reaction. (e) and (f) show these contributions as normalized values. HBcAg, Hepatitis B core antigen; MLR, multilinear regression; sfGFP, superfolder GFP

to identifying the process conditions to maximize product concentration. To assess the relative importance of each variable and their ability to predict the product concentration, four different types of MLR models were generated. These included linear, quadratic, interactions, and squared relationships. The linear models considered an intercept and a linear term for each predictor. The squared model additionally accounted for squared terms. The interaction model considered the intercept term, linear relationships and all product pairs of distinct predictors. The quadratic model was similar to the interaction model and additionally accounted for squared terms of each predictor.

The relative importance of each variable was assessed by initially building each of these MLR models using all the predictor variables (Time, Plas, Ext, pH and Temp) and then building a separate model with one of these predictor variables removed. The difference in the prediction ability of each of these models enables the relative importance of each variable to be defined. This systematic approach was performed for the four different MLR models (linear, quadratic, polynomial, and interactions). Evaluating the difference in the root mean square error between these models enabled the relative contribution of each variable on titer to be quantified. An example of a quadratic model to predict the titers for sfGFP is shown in Figure 5a while the one for HBcAg is shown in Figure 5b. The exact experiments used for Figure 5a are shown in Table 2 and those for Figure 5b are shown in Table 3. The MLR inputs used all predictor variables and were converted to coded factors to enable easier comparison of the coefficients shown in Figure 5c,d. The relative importance of each input variable for this MLR model is determined by the magnitude of the coefficient with sign indicating where there is a positive or negative relationship between the input variable and product concentration. Within the univariate analysis, the coefficient of determination,  $R^2$  was 0.78 for sfGFP and 0.70 for HBcAg. Equations for the MLR models shown in Figure 5 A–D of each product are shown below:

$$\text{sfGFP concentration} \sim 0.45 + 0.63\text{Time} + 0.92\text{Plas} + 0.33\text{Ext} - 0.54\text{pH} + 0.28\text{Temp} - 0.13\text{Time}^2 - 0.17\text{Plas}^2 - 0.09\text{Ext}^2 + 0.06\text{pH}^2 - 0.12\text{Temp}^2$$

$$\text{HBcAg concentration} \sim 0.65 + 0.34\text{Time} + 1.40\text{Plas} + 0.38\text{Ext} + 0.16\text{pH} + 0.12\text{Temp} - 0.12\text{Time}^2 - 0.36\text{Plas}^2 - 0.10\text{Ext}^2 - 0.09\text{Temp}^2$$

A summary of the averaged contributions of each variable on product concentration calculated as previously described is shown in Figure 5e,f for the sfGFP and HBcAg, respectively. The pH of the concentrated reaction mix and temperature were shown to have the largest influence on the final concentration of the sfGFP and the plasmid concentration, temperature and amount of extract were found to have the largest influence on the HBcAg.

To validate the importance of the interactions of these parameters, a face-centered response surface DoE was performed varying these selected variables. For the sfGFP, the pH was varied between 5.5 and 6.5 and the temperature between 32°C and 36°C. The titers generated by this DoE resulted in similar high sfGFP concentrations to those shown in Figure 4 and validated that low pH (5.5) and higher temperatures (34–36°C) resulted in maximal titers. These new conditions gave a titer of 686 µg/ml, a 38% increase from the typical reaction conditions (pH 6.8, 30°C, 6.1 nM (10 µg/ml) plasmid, 20% vol/vol non-induced BL21 Star™ (DE3) cell extract, and 4 hr) which resulted in titers of 497 µg/ml. The design of this set of experiments and the resulting contour plot based on interpolating the experimental product concentration between the experimental pH and temperature ranges can be seen in Supplementary Figure 1. The contour plots shown are generated by interpolating the experimental product concentration between the experimental pH and temperature ranges investigated. For the HBcAg, the three variables manipulated by the DoE were the plasmid concentration (3.8–11.5 nM [15–45 µg/ml]), amount of extract (15–25% vol/vol) and temperature (32–36°C). The experiments generated by this DoE resulted in significantly higher titers than previous experiments with the maximum found at a temperature of 32°C, a plasmid concentration of 45 µg/ml and an extract concentration of 25% vol/vol. This titer was almost triple the previous highest titer and demonstrates the importance of performing such a titer improvement exercise. Here we see a titer of 386 µg/ml, a 190% increase in titer from 133 µg/ml, which is achieved with the typical reaction conditions (pH 6.0, 30°C, 2.6 nM (10 µg/ml) plasmid, 20% vol/vol IPTG-induced BL21 Star™ (DE3) cell extract, and 4 hr). Another group used a modified A19 extract and 12 nM plasmid (where the gene of interest was in a pET24a backbone) to generate similar titers.<sup>24</sup> The face-centered central composite DoE and results can be seen in Supplementary Figure 2.

**TABLE 2** Experimental conditions for reactions producing sfGFP used for MVDA in Figure 5(a)

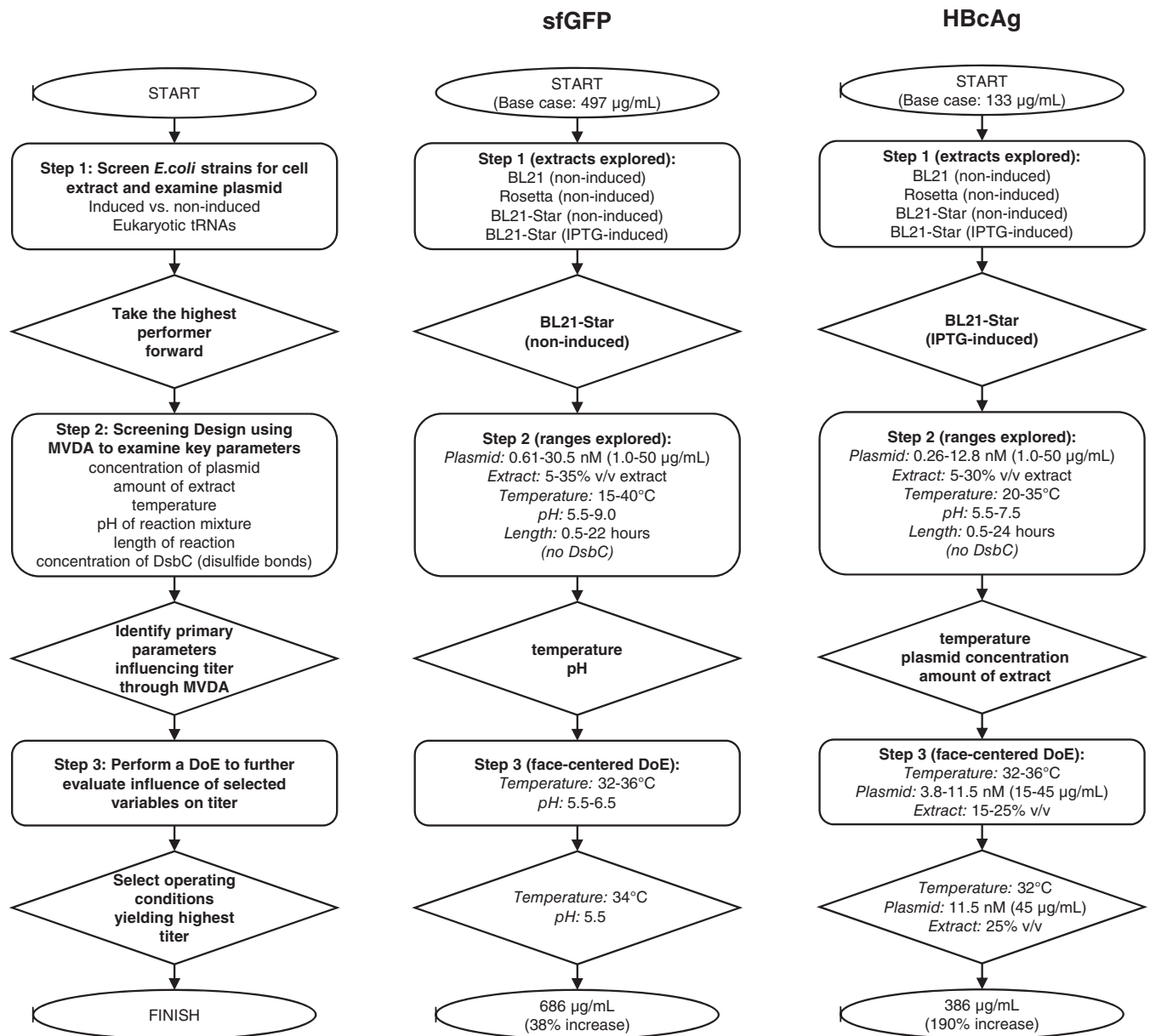
Experiment	Reaction length (hrs)	Plasmid concentration (µg/ml)	Plasmid concentration (nM)	Extract (% vol/vol)	pH of concentrated reaction mixture	Temperature (°C)	Product concentration (µg/ml)
1–24	4	10	6.1	20	6.8	15–40	16–673
25–51	4	10	6.1	20	5.5–9.0	30	96–757
52–72	4	10	6.1	5–35	6.8	30	30–555
73–87	4	1–50	0.61–30.5	20	6.8	30	100–482
88–105	0.5–22	10	6.1	20	6.8	30	141–523

Abbreviations: MVDA, multivariate data analysis; sfGFP, superfolder GFP.

**TABLE 3** Experimental conditions for reactions producing HBcAg used for MVDA in Figure 5(b)

Experiment	Reaction length (hr)	Plasmid concentration ( $\mu\text{g/ml}$ )	Plasmid concentration (nM)	Extract (% vol/vol)	pH of concentrated reaction mixture	Temperature ( $^{\circ}\text{C}$ )	Product concentration ( $\mu\text{g/ml}$ )
1-10	4	10	2.6	20	6.0	20-35	48-167
11-18	4	10	2.6	20	5.5-7.5	30	111-209
19-28	4	10	2.6	5-30	6.0	30	3-190
29-36	4	1-50	0.26-12.8	20	6.0	30	37-221
37-48	0.5-24	10	2.6	20	6.0	30	70-178

Abbreviations: HBcAg, Hepatitis B core antigen; MVDA, multivariate data analysis.

**FIGURE 6** Flow chart of recommended process development strategy for *Escherichia coli* CFPS reactions. CFPS, cell-free protein synthesis

The maximum titer for both products is located at the edge of the design space suggesting titer could be further improved and optimized by widening the experimental design space considered in this work. However, it is not our intention to optimize titer in this work, merely to demonstrate the advantages of our systematic process development approach, as summarized in the following section, and to maximize titer within a given design space. It is also important to mention that expanding the design space could have other unintended consequences. For example, the optimum titer of HBcAg expression may be achieved with increased amounts of plasmid and extract, but significantly increasing the presence of these components in the reaction also increases the cost of the reaction.

### 3.6 | Recommended process development method

Based on our findings, we have created a recommended process development strategy for the maximization of titer in CFPS reactions (Figure 6). We suggest determining the appropriate cell extract first before considering any other parameters. The cell extract has the most significant impact on product titer. While the use of the BL21 Star™ (DE3) extract resulted in high titers for the two products we examined, other groups have used a variety of other extracts—including BL21 (DE3) and Rosetta (DE3)—to successfully express protein.<sup>71,72</sup> In addition, depending on the protein of interest, there are a number of other strains that might have properties that would be beneficial for the protein, for example, the use of amber-less strains when producing proteins with non-natural amino acids. Also, optimization of the concentrated reaction mix for a particular product was not explored in this work, but based on previous examples, may also be beneficial for significantly increasing product titers.<sup>29,30,73,74</sup> Next, we recommend evaluating the influence of process parameters, changed in isolation, on titer and the application of MVDA to quantify the impact of those parameters. Subsequently the parameters with the highest influence on titer can be further investigated through a DoE approach. With proper planning, this process development strategy can be completed in under 48 hr.

## 4 | CONCLUSION

CFPS allows for recombinant protein production over short reaction times in small reaction volumes; we are therefore able to deploy a process development strategy that could be completed in under 48 hr. We determined that the most critical parameter is the *E. coli* strain chosen for the cell extract. Beyond that, titer can be incrementally increased by manipulating other process parameters. This method can be easily applied to new or difficult-to-express products in addition to efficiently testing a wide range of reaction conditions. We recommend first examining a series of extracts from different *E. coli* strains and observing the effects of IPTG-induction where possible before conducting further experiments on other parameters (Figure 6). Subsequently, MVDA modelling should be applied to

determine the influence of process parameters on production. Then, a DoE study should be used to identify the process conditions that result in the highest titer in the design space. Using this strategy, we were able to increase sfGFP and HBcAg titers by 38 and 190%, respectively, beyond the standard conditions.

We recommend this method over an initial scouting DoE due to the multitude of parameters that can be manipulated in CFPS reactions. Here we examined extract strain, concentrated reaction mix composition, plasmid selection, plasmid concentration, amount of extract, pH of the concentrated reaction mix, reaction temperature, and length of reaction. Depending on the product, other parameters like chaperone concentration, agitation rate, T7 RNA polymerase concentration, osmolality of the concentrated reaction mix, or protease inhibitor addition could also be critical for improving titer. While an initial DoE study to examine all these parameters could easily be performed given the high-throughput nature of CFPS, many parameters would not be critical to improving titer and the CFPS reactions in which those parameters are manipulated would be a waste of time and resources. By using MVDA to determine the parameters with the highest influence on titer, we can rule out other parameters and take a DoE approach that focuses only on the most critical parameters.

### ACKNOWLEDGMENTS

We would like to acknowledge Mark Turmaine for his assistance with TEM imaging and Haonan Xu for his assistance with GFP titer determination. pJL1 was a gift from Michael Jewett (Addgene plasmid # 69496; <http://n2t.net/addgene:69496>; RRID:Addgene\_69496) and pET14b-GFP was a gift from Martin Warren. Funding from the UK Engineering and Physical Sciences Research Council (EPSRC) for the Future Targeted Healthcare Manufacturing Hub is gratefully acknowledged (EP/P006485/1). Financial and in-kind support from the consortium of industrial users and sector organizations is also acknowledged. NAC was supported by the UCL Overseas Research Scholarship and the UCL Graduate Research Scholarship.

### CONFLICT OF INTEREST

W. R. is the CEO of iQur Limited.

### PEER REVIEW

The peer review history for this article is available at <https://publons.com/publon/10.1002/btpr.3062>.

### ORCID

Noelle Colant  <https://orcid.org/0000-0003-4832-5341>

Daniel G. Bracewell  <https://orcid.org/0000-0003-3866-3304>

### REFERENCES

1. Nirenberg MW, Matthaei JH. The dependence of cell-free protein synthesis in *E. coli* upon naturally occurring or synthetic polyribonucleotides. *Proc Natl Acad Sci U S A*. 1961;47(10):1588-1602.
2. Bundy BC, Hunt JP, Jewett MC, et al. Cell-free biomanufacturing. *Curr Opin Chem Eng*. 2018;22:177-183.
3. Shimizu Y, Ueda T. PURE technology. *Methods Mol Biol*. 2009;607:11-21.

4. Zemella A, Thoring L, Hoffmeister C, Kubick S. Cell-free protein synthesis: pros and cons of prokaryotic and eukaryotic systems. *ChemBiochem*. 2015;16:2420-2431.
5. Buntru M, Vogel S, Stoff K, Spiegel H, Schillberg S. A versatile coupled cell-free transcription-translation system based on tobacco BY-2 cell lysates. *Biotechnol Bioeng*. 2014;112:867-878.
6. Aw R, Polizzi K. Biosensor-assisted engineering of a high-yield *Pichia pastoris* cell-free protein synthesis platform. *Biotechnol Bioeng*. 2019;116(3):656-666.
7. Underwood KA, Swartz JR, Puglisi JD. Quantitative polysome analysis identifies limitations in bacterial cell-free protein synthesis. *Biotechnol Bioeng*. 2005;91(4):425-435.
8. Caschera F, Noireaux V. Synthesis of 2.3 mg/ml of protein with an all *Escherichia coli* cell-free transcription-translation system. *Biochimie*. 2014;99:162-168.
9. Knapp KG, Goerke AR, Swartz JR. Cell-free synthesis of proteins that require disulfide bonds using glucose as an energy source. *Biotechnol Bioeng*. 2007;97(4):901-908.
10. Schoborg JA, Hershewe JM, Stark JC, et al. A cell-free platform for rapid synthesis and testing of active oligosacaryltransferases. *Biotechnol Bioeng*. 2018;115:739-750.
11. Hong SH, Kwon YC, Jewett MC. Non-standard amino acid incorporation into proteins using *Escherichia coli* cell-free protein synthesis. *Front Chem*. 2014;2(34):1-7.
12. Zawada JF, Yin G, Steiner AR, et al. Microscale to manufacturing scale-up of cell-free cytokine production—a new approach for shortening protein production development timelines. *Biotechnol Bioeng*. 2011;108(7):1570-1578.
13. Salehi ASM, Smith MT, Bennett AM, Williams JB, Pitt WG, Bundy BC. Cell-free protein synthesis of a cytotoxic cancer therapeutic: onconase production and a just-add-water cell-free system. *Biotechnol J*. 2016;11:274-281.
14. Georgi V, Georgi L, Blechert M, et al. On-chip automation of cell-free protein synthesis: new opportunities due to a novel reaction mode. *Lab Chip*. 2016;16:269-281.
15. Stech M, Quast RB, Sachse R, Schulze C, Wustenhagen DA, Kubick S. A continuous-exchange cell-free protein synthesis system based on extracts from cultured insect cells. *PLoS One*. 2014;9:e96635.
16. Sutro Initiates First Clinical Trial of CD74-Targeting ADC for Lymphoma and Multiple Myeloma Treatment; The First of a New Generation of Precisely Engineered ADCs. 2018. <https://www.sutro.bio.com/sutro-initiates-first-clinical-trial-of-cd74-targeting-adc-for-lymphoma-the-first-of-a-new-generation-of-precisely-engineered-adcs/>. Accessed April 26.
17. Pardee K, Green AA, Takahashi MK, et al. Rapid, low-cost detection of Zika virus using programmable biomolecular components. *Cell*. 2016;165(5):1255-1266.
18. Pardee K, Green AA, Ferrante T, et al. Paper-based synthetic gene networks. *Cell*. 2014;159:940-954.
19. Jiang L, Zhao J, Lian J, Xu Z. Cell-free protein synthesis enabled rapid prototyping for metabolic engineering and synthetic biology. *Synth Syst Biol*. 2018;3:90-96.
20. Castan A, Schulz P, Wenger T, Fischer S. Cell Line Development. *Biopharmaceutical Processing: Development, Design, and Implementation of Manufacturing Processes*. Amsterdam, Netherlands: Elsevier; 2018: 131-146.
21. Schinn SM, Broadbent A, Bradley WT, Bundy BC. Protein synthesis directly from PCR: progress and applications of cell-free protein synthesis with linear DNA. *N Biotechnol*. 2016;33(4):480-487.
22. Tabor S. Expression using the T7 RNA polymerase/promoter system. *Curr Protoc Mol Biol*. 1990;11(1):1-11.
23. Jin X, Hong SH. Cell-free protein synthesis for producing 'difficult-to-express' proteins. *Biochem Eng J*. 2018;138:156-164.
24. Bundy BC, Franciszkowicz MJ, Swartz JR. *Escherichia coli*-based cell-free synthesis of virus-like particles. *Biotechnol Bioeng*. 2008;100(1): 28-37.
25. Sheng J, Lei S, Yuan L, Feng X. Cell-free protein synthesis of norovirus virus-like particles. *RSC Adv*. 2017;7:28837.
26. Farewell A, Neidhardt FC. Effect of temperature on in vivo protein synthetic capacity in *Escherichia coli*. *J Bacteriol*. 1998;180(17):4704-4710.
27. Schumann W, Ferreira LCS. Production of recombinant proteins in *Escherichia coli*. *Genet Mol Biol*. 2004;27(3):442-453.
28. Kim DM, Swartz JR. Prolonging cell-free protein synthesis with a novel ATP regeneration system. *Biotechnol Bioeng*. 1999;66(3):180-188.
29. Cai Q, Hanson JA, Steiner AR, et al. A simplified and robust protocol for immunoglobulin expression in *Escherichia coli* cell-free protein synthesis systems. *Biotechnol Prog*. 2015;31(3):823-831.
30. Dopp JL, Tamiev DD, Reuel NF. Cell-free supplement mixtures: elucidating the history and biochemical utility of additives used to support in vitro protein synthesis in *E. coli* extract. *Biotechnol Adv*. 2019;37(1): 246-258.
31. Dopp JL, Reuel NF. Process optimization for scalable *E. coli* extract preparation for cell-free protein synthesis. *Biochem Eng J*. 2018;138: 21-28.
32. Goerke AR, Swartz JR. Development of cell-free protein synthesis platforms for disulfide bonded proteins. *Biotechnol Bioeng*. 2008;99 (2):351-367.
33. Yin G, Garces ED, Yang J, et al. Aglycosylated antibodies and antibody fragments produced in a scalable in vitro transcription-translation system. *MAbs*. 2012;4(2):217-225.
34. Hong SH, Kwon YC, Martin RW, et al. Improving cell-free protein synthesis through genome engineering of *Escherichia coli* lacking release factor 1. *ChemBiochem*. 2015;16(5):844-853.
35. Failmezger J, Rauter M, Nitschel R, Kraml M, Siemann-Herzberg M. Cell-free protein synthesis from non-growing, stressed *Escherichia coli*. *Nat Sci Rep*. 2017;7(16524):1-10.
36. Wilding KM, Hunt JP, Wilkerson JW, et al. Endotoxin-free *E. coli*-based cell-free protein synthesis: pre-expression endotoxin removal approaches for on-demand cancer therapeutic production. *Biotechnol J*. 2019;14(3):1-6.
37. Zawada J, Swartz J. Effects of growth rate on cell extract performance in cell-free protein synthesis. *Biotechnol Bioeng*. 2006;94(4): 618-624.
38. Levine MZ, So B, Mullin AC, Watts KR, Oza JP. Redesigning upstream processing enables a 24-hour workflow from *E. coli* cells to cell-free protein synthesis. *bioRxiv*. 2019. <https://doi.org/10.1101/729699>.
39. Bremer H, Dennis PP. Modulation of chemical composition and other parameters of the cell at different exponential growth rates. *EcoSal Plus*. 2008;3(1). <http://dx.doi.org/10.1128/ecosal.5.2.3>.
40. Kwon YC, Jewett MC. High-throughput preparation methods of crude extract for robust cell-free protein synthesis. *Nat Sci Rep*. 2015; 5(8663):1-8.
41. Caschera F, Noireaux V. A cost-effective polyphosphate-based metabolism fuels an all *E. coli* cell-free expression system. *Metab Eng*. 2015;27:29-37.
42. Jewett MC, Swartz JR. Mimicking the *Escherichia coli* cytoplasmic environment activates long-lived and efficient cell-free protein synthesis. *Biotechnol Bioeng*. 2004;86(1):19-26.
43. Jewett MC, Calhoun KA, Voloshin A, Wu JJ, Swartz JR. An integrated cell-free metabolic platform for protein production and synthetic biology. *Mol Syst Biol*. 2008;4:220.
44. Expressway™ Cell-Free *E. coli* Expression System. 2011. [https://assets.thermofisher.com/TFS-Assets/LSG/manuals/expressway\\_system\\_man.pdf](https://assets.thermofisher.com/TFS-Assets/LSG/manuals/expressway_system_man.pdf). Accessed September 27.
45. Evrogen. Green fluorescent protein TurboGFP. [http://evrogen.com/products/TurboGFP/TurboGFP\\_Detailed\\_description.shtml](http://evrogen.com/products/TurboGFP/TurboGFP_Detailed_description.shtml). Published 2020. Accessed.
46. FPbase. Superfolder GFP. <https://www.fpbase.org/protein/superfolder-gfp/>. Published 2020. Accessed.
47. FPbase. Folding Reporter GFP. 2020.

48. Bird LE, Rada H, Verma A, Gasper R, Birch J, Jennions M, Löwe J, Moraes I, Owens RJ. Green fluorescent protein-based expression screening of membrane proteins in *Escherichia coli*. *J Vis Exp*. 2015;(95). <http://dx.doi.org/10.3791/52357>.
49. Ramirez A, Morris S, Maucourant S, et al. A virus-like particle vaccine candidate for influenza A virus based on multiple conserved antigens presented on hepatitis B tandem core particles. *Vaccine*. 2018;36(6):873-880.
50. Chizzolini F, Forlin M, Martin NY, Berloff G, Cecchi D, Mansy SS. Cell-free translation is more variable than transcription. *ACS Synth Biol*. 2017;6:638-647.
51. Iskakova MB, Szaflarski W, Dreyfus M, Remme J, Nierhaus KH. Troubleshooting coupled in vitro transcription-translation system derived from *Escherichia coli* cells: synthesis of high-yield fully active proteins. *Nucleic Acids Res*. 2006;34(19):e135.
52. Jewett MC, Hodgman CE, Gan R, Inventors. Methods for cell-free protein synthesis. US patent 95281372016.
53. Jewett MC, Martin RW, Hong SH, Kwon YC, Des Soye BJ, Inventors. Methods for improved in vitro protein synthesis with proteins containing non standard amino acids. US patent 201600603012016.
54. Pedelacq JD, Cabantous S, Tran T, Terwillinger TC, Waldo GS. Engineering and characterization of a superfolder green fluorescent protein. *Nat Biotechnol*. 2006;24(1):79-88.
55. Overkamp W, Beilharz K, Detert Oude Weme R, et al. Benchmarking various green fluorescent protein variants in *Bacillus subtilis*, *Streptococcus pneumoniae*, and *Lactococcus lactis* for live cell imaging. *Appl Environ Microbiol*. 2013;79(20):6481-6490.
56. Strychalski EA, Romantseva EF. CELL-FREE (Comparable Engineered Living Lysates for Research Education and Entrepreneurship) Workshop Report. 2020.
57. Wang PH, Fujishima K, Berhanu S, et al. A single polyphosphate kinase-based ntp regeneration system driving cell-free protein synthesis. *ChemRxiv*. 2019. <https://doi.org/10.26434/chemrxiv.8874410.v2>.
58. Doron N. Bacterial strains for protein production. *The Wolfson Centre for applied structural biology at the Hebrew University of Jerusalem*. The Hebrew University of Jerusalem; 2015. <http://wolfson.huji.ac.il/expression/bac-strains-prot-exp.html>.
59. Studier FW, Moffat BA. Use of bacteriophage T7 RNA polymerase to direct selective high-level expression of cloned genes. *J Mol Biol*. 1986;189(1):113-130.
60. Silverman AD, Kelley-Loughnane N, Lucks JB, Jewett MC. Deconstructing cell-free extract preparation for in vitro activation of transcriptional genetic circuitry. *ACS Synth Biol*. 2019;8(2):403-414.
61. Dopp JL, Jo YR, Reuel NF. Methods to reduce variability in *E. coli*-based cell-free protein expression. *Synth Syst Biotech*. 2019;4(4):204-211.
62. Doerr A, de Reus E, van Nies P, et al. Modelling cell-free RNA and protein synthesis with minimal systems. *Phys Biol*. 2019;16(2):025001.
63. Nagaraj VH, Greene JM, Sengupta M, Sontag ED. Translation inhibition and resource balance in the TX-TL cell-free gene expression system. *Synth Biol*. 2017;2(1). <http://dx.doi.org/10.1093/synbio/ysx005>.
64. de Groot NS, Ventura S. Effect of temperature on protein quality in bacterial inclusion bodies. *FEBS Lett*. 2006;580(27):6471-6476.
65. Caschera F, Noireaux V. Preparation of amino acid mixtures for cell-free expression systems. *BioTechniques*. 2015;58(1). <http://dx.doi.org/10.2144/000114249>.
66. Roberts TM, Rudolf F, Meyer A, Pellaux R, Whitehead E, Panke S, Held M. Identification and Characterisation of a pH-stable GFP. *Scientific Reports*. 2016;6(1). <http://dx.doi.org/10.1038/srep28166>.
67. Stepanenko OV, Stepanenko OV, Kuznetsova IM, Verkhusha VV, Turoverov KK. Sensitivity of superfolder GFP to ionic agents. *PLoS One*. 2014;9(10):e110750.
68. Stark JC, Huang A, Nguyen PQ, et al. BioBits bright: a fluorescent synthetic biology education kit. *Sci Adv*. 2018;4(8):1-10.
69. Kim DM, Choi CY. A semicontinuous prokaryotic coupled transcription/translation system using a dialysis membrane. *Biotechnol Prog*. 1996;12:645-649.
70. Goldrick S, Sandner V, Cheeks M, et al. Multivariate data analysis methodology to solve data challenges related to scale-up model validation and missing data on a micro-bioreactor system. *Biotechnol J*. 2020;15(3):1800684.
71. Chumpolkulwong N, Hori-Takemoto C, Hosaka T, et al. Effects of *Escherichia coli* ribosomal protein S12 mutations on cell-free protein synthesis. *Eur J Biochem*. 2004;271(6):1127-1134.
72. Kim TW, Keum JW, Oh IS, Choi CY, Park CG, Kim DM. Simple procedures for the construction of a robust and cost-effective cell-free protein synthesis system. *J Biotechnol*. 2006;126(4):554-561.
73. Kai L, Dotsch V, Kaldenhoff R, Bernhard F. Artificial environments for the co-translational stabilization of cell-free expressed proteins. *PLoS One*. 2013;8(2):e56637.
74. Pederson A, Hellberg K, Enberg J, Karlsson BG. Rational improvement of cell-free protein synthesis. *N Biotechnol*. 2011;28:218-224.

## SUPPORTING INFORMATION

Additional supporting information may be found online in the Supporting Information section at the end of this article.

**How to cite this article:** Colant N, Melinek B, Teneb J, et al. A rational approach to improving titer in *Escherichia coli*-based cell-free protein synthesis reactions. *Biotechnol Progress*. 2020; e3062. <https://doi.org/10.1002/btpr.3062>